1 # Supplementary Materials for

3 # Formation of Reactive Nitrogen Species Promoted by Iron
4 # Ions Through the Photochemistry of Neonicotinoid
5 # Insecticide

7 Zhu Ran[1,2], Yanan Hu[1,2,3*], Yuanzhe Li[1,2], Xiaoya Gao[1,2], Can Ye[4], Shuai Li[5], Xiao Lu[5],
8 Yongming Luo[1,2,3], Sasho Gligorovski [6,7,8*], Jiangping Liu[1,2*]

10

11 [1]Faculty of Environmental Science and Engineering, Kunming University of Science and Technology,
12 Kunming 650500, China;
13 [2]The Innovation Team for Volatile Organic Compounds Pollutants Control and Resource Utilization of
14 Yunnan Province, The Higher Educational Key Laboratory for Odorous Volatile Organic Compounds
15 Pollutants Control of Yunnan Province, Kunming 650500, China;
16 [3]Faculty of Chemical Engineering, Kunming University of Science and Technology, Kunming 650500,
17 China;
18 [4]Faculty of Environmental Science and Engineering, Peking University, Beijing 100871, China;
19 [5]School of Atmospheric Sciences, Sun Yat-sen University, Southern Marine Science and Engineering
20 Guangdong Laboratory (Zhuhai), Zhuhai, Guangdong 519082, China;
21 [6]State Key Laboratory of Organic Geochemistry and Guangdong Provincial Key Laboratory of
22 Environmental Protection and Resources Utilization, Guangzhou Institute of Geochemistry, Chinese
23 Academy of Sciences, Guangzhou 510 640, China;
24 [7]Guangdong-Hong Kong-Macao Joint Laboratory for Environmental Pollution and
25 Control, Guangzhou Institute of Geochemistry, Chinese Academy of Science, Guangzhou 510640, China;
26 [8]Chinese Academy of Science, Center for Excellence in Deep Earth Science, Guangzhou, 510640, China.

27

28 *Correspondence*: (Sasho Gligorovski) gligorovski@gig.ac.cn; (Jiangping Liu) liujiangping18@
29 mails.ucas.ac.cn; (Yanan Hu) huyanan0917@163.com

30

31

32

 Supplementary Text

 Text S1. Ionic analysis at different Fe^{3+} concentrations

35 As depicted in Figure S2, the direct photolysis of NPM produced a large amount of NO_3^- and NO_2^- in the

36 absence of Fe^{3+}, and in the presence of Fe^{3+} restricted NO_3^- and NO_2^- production occurred, which was

37 consistent with the change of the photolysis rate constant of NPM. NO_2 produced by direct photolysis of

38 NPM is hydrolyzed in aqueous media to form NO_2^- and NO_3^-, and nitrogenous species are partially

39 dissolved during their release from the liquid to the gas phase. The reaction of NOx with $O_2^{-\bullet}$ radicals will

40 also produce NO_2^- and NO_3^-. The presence of Fe^{3+} provides a strong acid environment (Table S1) and the

41 protonation of NO_2^- will lead to the release of HONO (Lu et al., 2015; Wang et al., 2021). Upon

42 irradiation at $\lambda > 300$ nm, Fe^{3+} species (monomeric and dimeric) are known to undergo a redox process

43 giving rise to Fe(II) and $\bullet$OH radicals (Bai et al., 2023). Fe^{2+} cannot coexist with NO_3^-, and NO_2 gas will

44 be produced by redox reaction. In short, the addition of Fe^{3+} promotes the conversion of NO_3^- and NO_2^-

45 to HONO and NOx. In the presence of high Fe^{3+} concentration, the photolysis rate of NPM showed an

46 increasing trend, and $\bullet$OH and $O_2^{-\bullet}$ produced under light irradiation were more elevated than those

47 produced under low concentration of Fe^{3+} (Figure 2), which slightly promoted the generation of NO_3^-

48 and NO_2^-.

 Text S2. Global simulation of NOx and HONO fluxes

50 We developed the global inventory of the NPM-emitted NO_x and HONO fluxes. Gridded and hourly

51 downward solar radiation data are obtained from the Modern-Era Retrospective analysis for Research

52 and Application version 2 (MERRA-2) assimilated meteorological fields. We calculated the emission

53 flux for each model grid at a horizontal resolution of $0.5° \times 0.625°$ (consistent with MERRA2 radiation

54 dataset) following Eq-S1, but assuming that the environmental NPM concentration is three orders smaller

55 than the experimental conditions of 0.5 mg L^{-1}. We examined the relationship between HONO and NOx

56 formation and light intensity from the experimental results, at a fixed NPM concentration level (Figure

57 S5-S6). The parameterization of HONO and NOx productions from NPM photolysis at Fe^{3+}

58 concentration of 0.025 mg ml^{-1} used in our estimation is based on Eq-S1:

59 $Y_{HONO} = 1.58595 \times 10^{9} X - 1.19123 \times 10^{11}$, $Y_{NO2} = 6.58261 \times 10^{8} X - 1.81889 \times 10^{10}$, $Y_{NO} = 2.58054 \times 10^{8} X -$

60 1.41507×10^{10} $\qquad$ Eq-S1

61   where y represents the HONO/NOx fluxes, X represents the light density.

Table S1. Measured Photolysis Rate Constants (k) and Half-time ($T_{1/2}$) of NPM in aqueous solution at different Fe^{3+} concentrations.

The concentration of Fe^{3+} / mg.ml^{-1}	Kinetic equation	Rate Constants (k)/min^{-1}	Half-time ($T_{1/2}$)/min	R^2	Initial pH value
0	$C_t = 0.501e^{-0.00427t}$	0.00427	162.3	0.99438	7.3
0.1	$C_t = 0.477e^{-0.00382t}$	0.00382	181.5	0.98757	3.4
0.25	$C_t = 0.520e^{-0.00310t}$	0.00310	223.6	0.98065	2.9
0.5	$C_t = 0.514e^{-0.00346t}$	0.00346	200.3	0.98869	2.6
0.8	$C_t = 0.513e^{-0.00513t}$	0.00513	135.1	0.99064	2.4
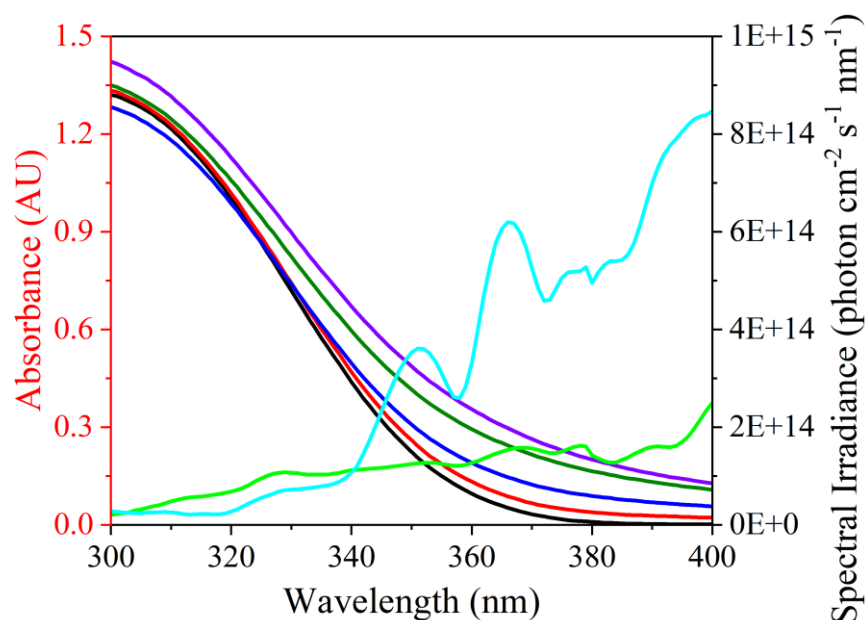
Figure S1. The absorption spectra of NPM (0.05 mg ml-1) in the absence of Fe^{3+} (dark line), and in the presence of different concentrations of Fe^{3+}: 0.01 mg ml^{-1} (red line), 0.025 mg ml^{-1} (blue line), 0.05 mg ml^{-1} (green line) and 0.08 mg ml^{-1} (purple line). Comparison of the spectral irradiance of the Xenon lamp (Fluorescent light blueed line) and the spectral irradiance of the sunlight (fluorescent light green line) measured by the spectroradiometer (HP350UVP, China). The spectral irradiance is determined for Kunming (latitude 24.85285, longitude 102.86016) on July 26 2022 at noon.
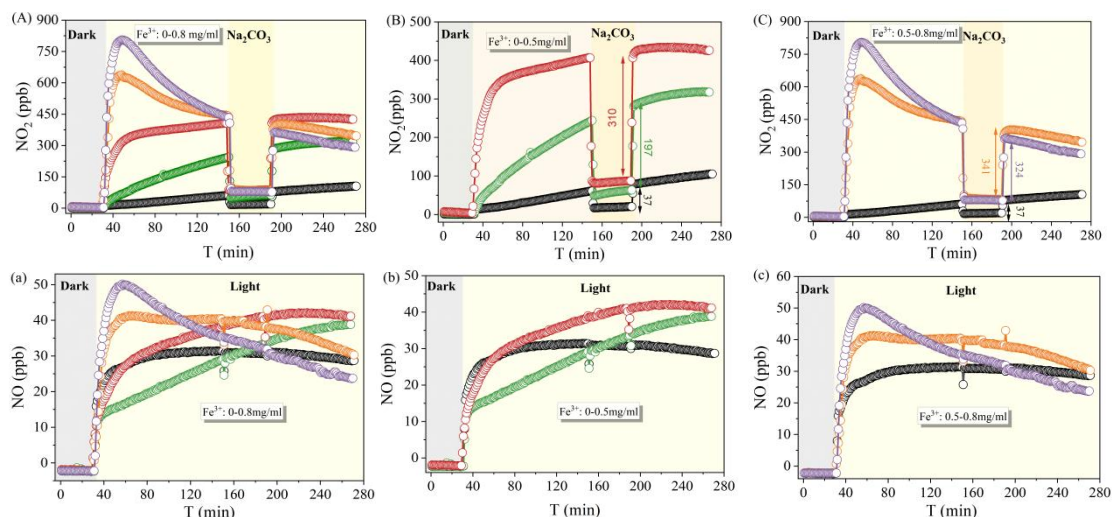
Figure S2. The temporal changes of NO_2, HONO and NO during the photolysis of NPM (0.5 mg ml^{-1}) in the absence of Fe^{3+} (dark line), and in the presence of different concentrations of Fe^{3+}: 0.1 mg ml^{-1} (blue line), 0.25 mg ml^{-1} (red line), 0.5 mg ml^{-1} (orange line) and 0.8 mg ml^{-1} (purple line). Reaction conditions: irradiation intensity of 169.4 W m^{-2} at 300-400 nm, temperature of 298 K.
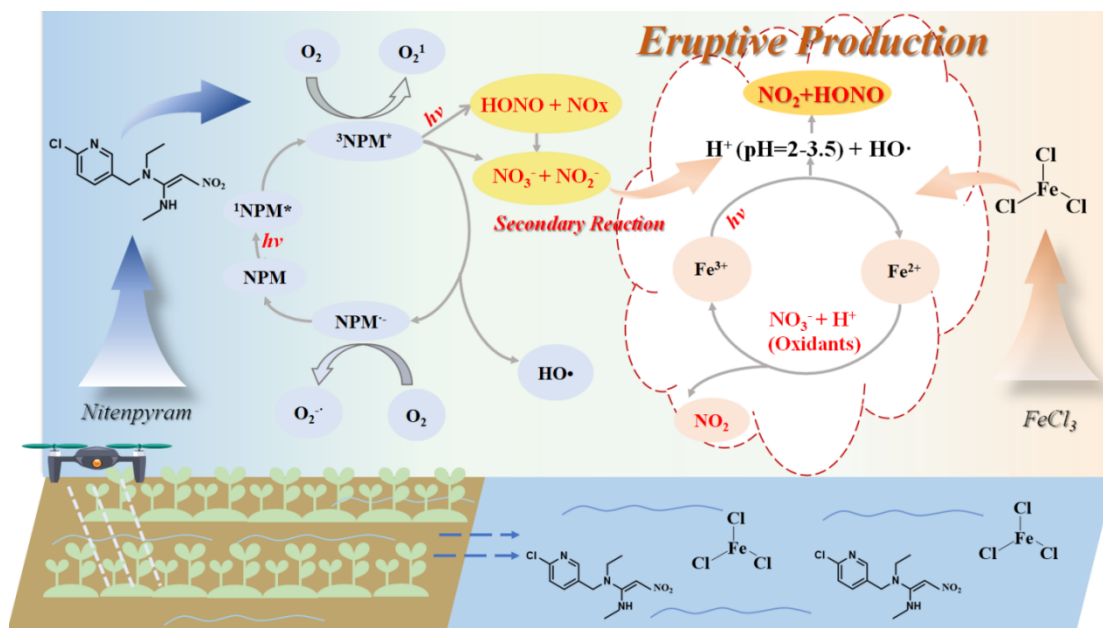
Figure S3. Proposed mechanism of NPM photolysis in the presence of iron ions leading to HONO and NOx formation.
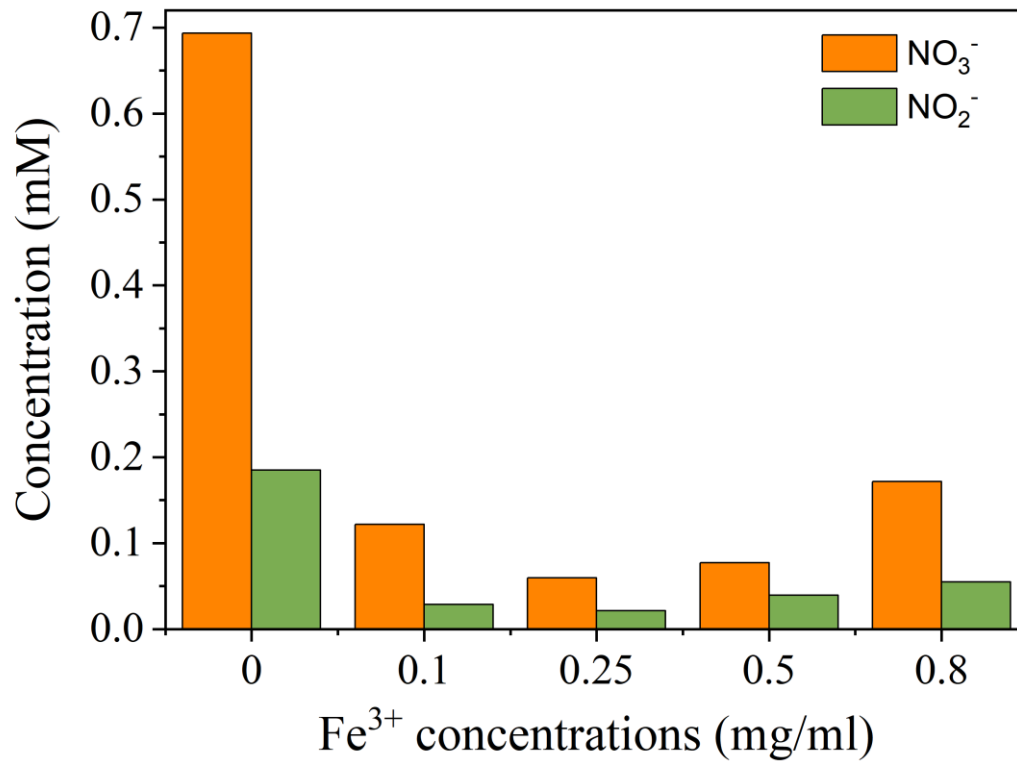
82

83

84 **Figure S4.** The nitrate and nitrite ions concentrations of NPM (0.5 mg ml^{-1}) by 2 hours photolysis at different
85 concentrations of Fe^{3+}.

86
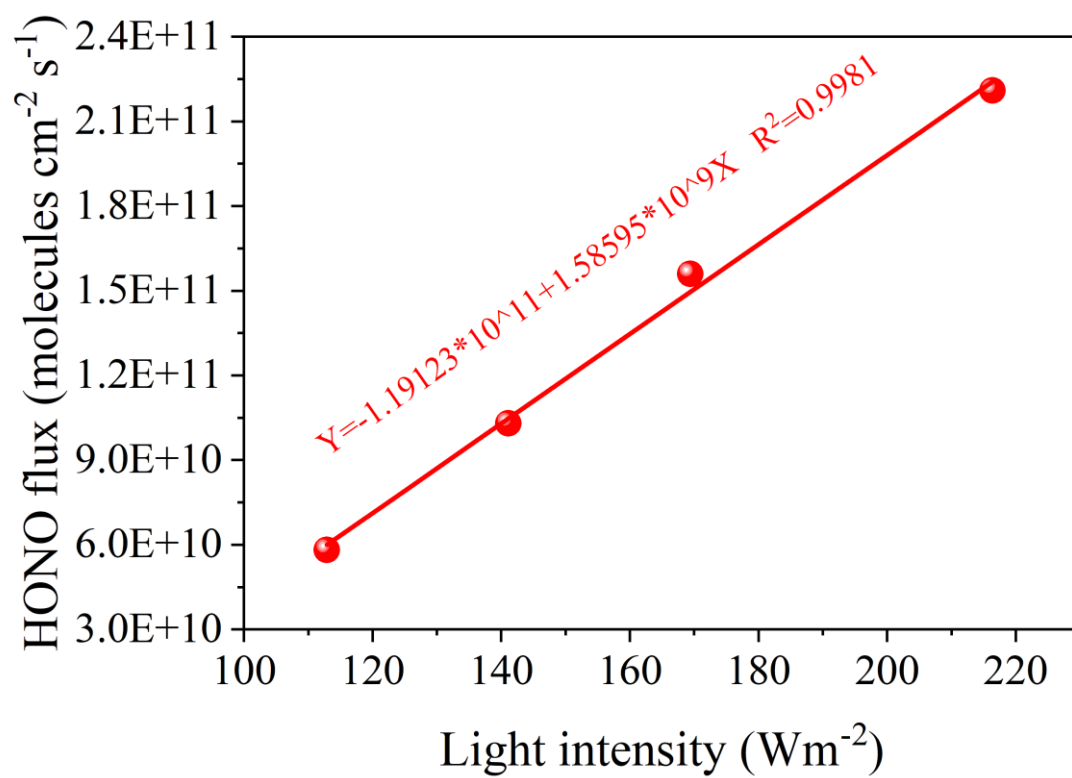
87

88

89 **Figure S5.** HONO flux from NPM photolysis under different light intensity. Conditions: NPM concentration of 0.05

90 mg ml-1, Fe^{3+} concentration of 0.025 mg ml^{-1}, irradiation time of 60 min, temperature of 298 K.

91
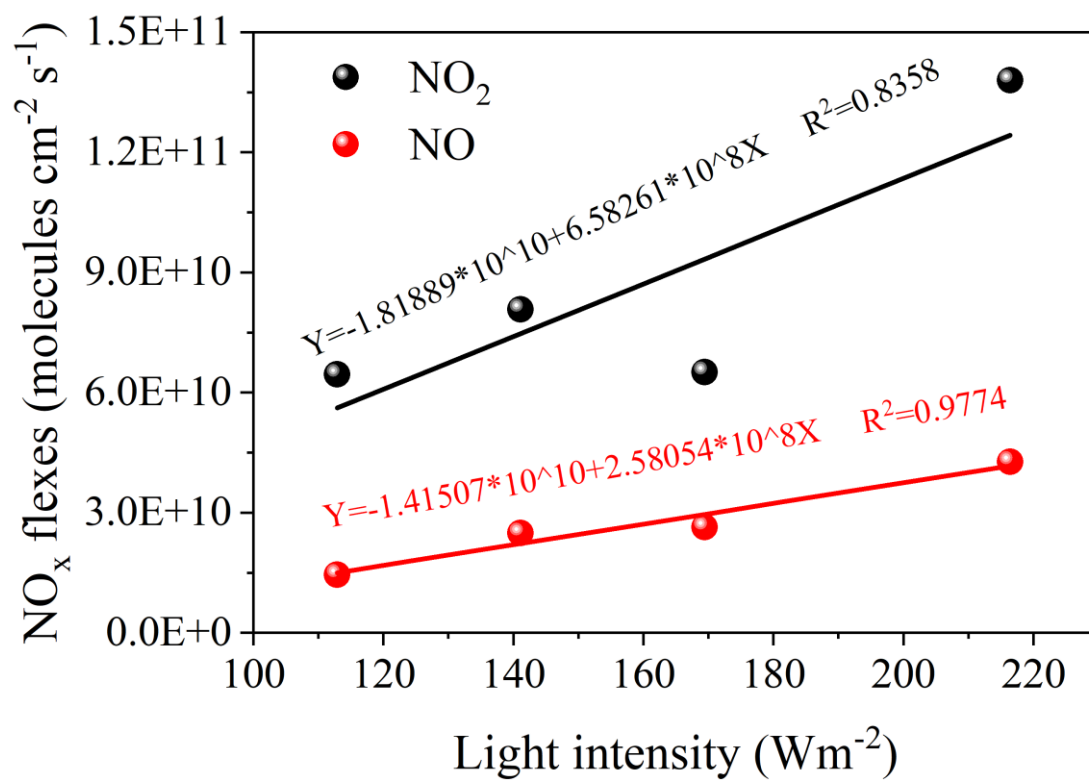
92

93

94 **Figure S6.** NOx flux from NPM photolysis under different light intensity. Conditions: NPM concentration of 0.05
95 mg ml^{-1}, Fe^{3+} concentration of 0.025 mg ml^{-1}, irradiation time of 60 min, temperature of 298 K.

96

References

Lu, Z., Challis, J. K., and Wong, C. S.: Quantum Yields for Direct Photolysis of Neonicotinoid Insecticides in Water: Implications for Exposure to Nontarget Aquatic Organisms, Environ. Sci. Technol. Lett., 2, 188-192, doi:10.1021/acs.estlett.5b00136, 2015.

100

Wang, Y., Huang, D. D., Huang, W., Liu, B., Chen, Q., Huang, R., Gen, M., Mabato, B. R. G., Chan, C. K., Li, X., Hao, T., Tan, Y., Hoi, K. I., Mok, K. M., and Li, Y. J.: Enhanced Nitrite Production from the Aqueous Photolysis of Nitrate in the Presence of Vanillic Acid and Implications for the Roles of Light-Absorbing Organics, Environ. Sci. Technol. Lett., 55, 15694-15704, doi:10.1021/acs.est.1c04642, 2021.

105

Bai, X., Yang, Q., Guo, Y., Hao, B., Zhang, R., Duan, R., and Li, J.: Alkyl halide formation from degradation of carboxylic acids in the presence of Fe(III) and halides under light irradiation, Water. Res., 235, doi:10.1016/j.watres.2023.119842, 2023.